http://dx.doi.org/10.5012/bkcs.2013.34.9.2685

Glucose Oxidation on Gold-modified Copper Electrode

Ji-Eun Lim, Sang Hyun Ahn,† Sung Gyu Pyo, Hyungbin Son,* Jong Hyun Jang,† and Soo-Kil Kim*

Department of Nano Bio Energy Engineering, School of Integrative Engineering, Chung-Ang University, Seoul 156-756, Korea
**E-mail: being@cau.ac.kr (H. S.); *E-mail: sookilkim@cau.ac.kr (S.-K. Kim)*
†Fuel Cell Research Center, Korea Institute of Science and Technology, Seoul 136-791, Korea
Received April 8, 2013, Accepted June 18, 2013

The activities of Au-modified Cu electrodes toward glucose oxidation are evaluated according to their fabrication conditions and physico-chemical properties. The Au-modified Cu electrodes are fabricated by the galvanic displacement of Au on a Cu substrate and the characteristics of the Au particles are controlled by adjusting the displacement time. From the glucose oxidation tests, it is found that the Au modified Cu has superior activity to the pure Au or Cu film, which is evidenced by the negative shift in the oxidation potential and enhanced current density during the electrochemical oxidation. Though the activity of the Au nanoparticles is a contributing factor, the enhanced activity of the Au-modified Cu electrode is due to the increased oxidation number of Cu through the electron transfer from Cu to more electronegative Au. The depletion of electron in Cu facilitates the oxidation of glucose. The stability of the Au-modified Cu electrode was also studied by chronoamperometry.

Key Words : Glucose, Bio fuel cell, Electrochemical oxidation, Catalyst

Introduction

The use of a disposable primary battery as a power source for implantable medical devices has some drawbacks, such as the necessity for the continuous monitoring of the battery function and surgical re-implantation of a fresh battery. For this reason, bio fuel cells (BFCs) using nutrients in the blood as a fuel are drawing continuous attention as a semi-permanent power source within the human body.[1,2] The early type of BFCs was composed of two electrodes immersed in an aqueous electrolyte, which are separated by a semi-permeable membrane. Microbes or enzymes immobilized on the electrodes act as catalysts for the oxidation of fuels and the electrons generated during the oxidation move to the cathode for use in the oxygen reduction at the cathode.[3,4] BFCs for implantable devices need to use fuels that are water-soluble, bio-compatible, and easy to obtain within the body, such as glucose.

Besides the BFCs application, the glucose oxidation has been studied for the development of glucose sensors. Deng *et al.* reported the electrochemistry of glucose oxidase using boron-doped carbon nanotubes modification.[5] Safavi *et al.* investigated the glucose oxidation reaction on $Ni(OH)_2$ modified carbon ionic liquid electrode for the purpose of fabrication of a non-enzymatic glucose sensors.[6] For non-enzymatic glucose sensing, Rong *et al.* also used Pt nanoparticles on carbon nanotubes for detecting glucose.[7] The combination of enzyme and non-enzymatic catalyst (copper oxide) for glucose biosensor was also reported by Luque *et al.*.[8]

In both cases of BFCs and glucose sensors, glucose is oxidized to gluconolactone, generating two electrons.[2] The oxidation reaction requires enzymes such as glucose oxidase.[2,5,8] However, enzymes are highly vulnerable to external shocks, such as changes in the chemical and thermal conditions, and lose their activities. R. Wilson *et al.* reported the deformation of the enzymes at temperatures higher than 40 °C and pHs lower than 2 or higher than 8.[9] In addition, enzymes have low electrical conductivity and suffer from poor efficiency for the conduction of generated electrons. Besides their vulnerability and low conductivity, the immobilization process of enzymes on the electrodes is further complicated by the complexity of the electrode structure and low stability.[7,10,11] Therefore, there is a growing necessity to substitute the enzyme with metal catalysts having high activity toward glucose oxidation and high stability.

There have been many studies into metal catalysts for glucose oxidation using single metals or binary and ternary alloys.[10-22] In more detail, several single metal catalysts using Au,[10,12,14-16,19,22] Pt,[10,12,16,18] Cu[10,20] and Ni[10,11,21] have been reported to have significant activities toward glucose oxidation. Particularly, Pt is a well-known catalyst for proton exchange membrane fuel cells and direct methanol fuel cells as both anode and cathode catalysts. In this sense, it has also been researched in the field of BFCs, though the high cost of Pt and its relatively low tolerance to poisoning by reaction intermediates during the glucose oxidation.[7,17]

Au, which is also a member of Pt group, is another candidate for catalysts having significant activity toward glucose oxidation. Besides the use of Au as a single metal, binary alloys based on Au have been widely investigated. C. Jin *et al.* found that Au-Pt alloy has high activity toward glucose oxidation at more negative potentials than pure Au.[13] Studies on Au-Ag, Au-Ru, Au-Pb, and Au-Cd alloy catalysts have also been reported.[14,15]

Besides the noble metal catalysts, Cu and Ni are also

known as metals having activity toward glucose oxidation. Non-noble metals normally have more positive onset potentials for glucose oxidation than Au or Pt, however the cheaper price of the former is a great advantage. H.B. Hassan *et al.* reported the enhanced activity of CuO toward glucose oxidation[20] and S.S. Mahshid *et al.* tested the validity of using Pt/Ni nanowire as a catalyst.[11] Combining of noble metal catalyst and non-noble metal catalyst in proper way, therefore, may have synergistic effects both in the reaction over-potential and the catalyst price.

In this study, we fabricated Au particle-modified Cu electrodes and tested their activity toward glucose oxidation for possible application to BFCs or glucose sensors. Among the various methods of synthesizing catalysts, such as impregnation,[23] colloidal synthesis,[24] electrodeposition,[25-27] and sputter deposition,[28,29] we used galvanic displacement deposition[30,31] to fabricate Au particles on a Cu substrate. In this reaction, the electrons generated during the dissolution of the Cu substrate were used in the deposition of Au particles. The morphology, shape and size, and surface coverage of the Au particles on the Cu substrate were easily controlled by adjusting the displacement conditions. The deposited Au particles may contribute to the enhancement of the activity toward glucose oxidation, either by their intrinsic activity or by affecting the physico-chemical properties of the underlying Cu substrate. The possible advantages of the suggested electrode may include the arithmetic sum of the individual catalyst activities (Au particles and the underlying Cu substrate) and the modulation of electronic structures caused by the electron transfer between the two metals. The activities of the fabricated electrodes were characterized using spectroscopic and electrochemical analysis and some mechanisms of glucose oxidation on the modified electrodes were suggested based on the results.

Experimental

Materials and Chemicals. Copper foil (thickness 0.25 mm, Sigma-Aldrich, 99.98%) and Gold(III) chloride hydrate ($HAuCl_4 \cdot xH_2O$, Sigma-Aldrich, 99.999%) were used as a substrate and an Au precursor for the displacement, respectively. The supporting electrolyte for the displacement was made from sodium chloride (NaCl, Daejung, 99%). D-(+)-Glucose ($C_6H_{12}O_6$, Sigma-Aldrich) and sodium hydroxide (NaOH, Daejung, 98%) were used for the glucose oxidation.

Preparation of Electrodes. Au-modified Cu electrodes were prepared by immersing Cu foil in an aqueous solution containing 3 mM of gold(III) chloride hydrate and 0.5 M sodium chloride for different reaction times of 10s, 25s, 45s, and 1 min. Au particles are deposited on the Cu foil by displacement reactions; $2Au^{3+} + 6e^- \rightarrow 2Au$ (reduction) *vs.* $3Cu \rightarrow 3Cu^{2+} + 6e^-$ (oxidation). The Au-deposited Cu electrodes were then washed in an ultrasonic bath for 30s, followed by drying in an N_2 stream. For comparison, a 120 nm thick Au film was also deposited on Cu foil by sputter deposition. A DC-Sputter (PSPD-0710, PS TEK) was used and the Au film was deposited at a DC power of 1 kW for 30s under a base pressure of 5.5×10^{-3} torr.

Characterization of the Electrodes. The morphology, size, and coverage of the Au-modified Cu electrodes were observed by Field Emission Scanning Electron Microscopy (FE-SEM, SIGMA/Carl Zeiss). An Electron Probe Micro Analyzer (EPMA, JEOL JXA-8500F) was used to map the distribution of Au particles on Cu. The electrocatalytic activities of the Au-modified Cu electrodes toward glucose oxidation were observed using cyclic voltammetry (CV) and chronoamperometry (CA). A three-electrode cell system attached to a potentiostat/galvanostat (Autolab, PGSTAT302F) was used in all of the electrochemical measurements. A saturated calomel electrode (SCE) and Pt wire were used as the reference electrode and counter electrode, respectively. CV was conducted in the potential range from −1.0 V to 1.0 V with a scan rate of 50 mV/s in an electrolyte composed of 0.3 M NaOH and various concentrations of glucose (0 mM, 5 mM, 10 mM, 15 mM, 30 mM). CA was performed at 0.6 V *vs*. SCE for 3600s and 0.3 M NaOH + 10 mM glucose solution was used as the electrolyte. All of the electrolytes were purged with N_2 gas for 30 min to remove any dissolved gas prior to the electrochemical tests.

Results and Discussion

Figure 1 presents the FE-SEM images of the bare Cu foil and Au-deposited Cu electrodes used in the study. The surface of the bare Cu foil (Fig. 1(a)) consists of sparsely distributed grooves and steps having dimensions of several tens of nm. Voids or pinholes are also observed on the rough surface. Once the Cu surface was covered with the sputter deposited Au thin film (Fig. 1(b)), most of the grooves or steps were buried and only a few pinholes remained, giving

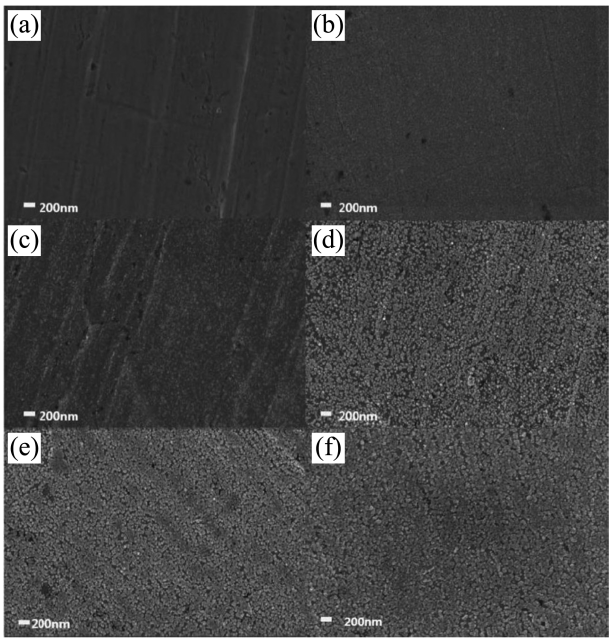

Figure 1. FESEM images of Cu foil (a), sputter deposited Au film on Cu (b), displacement deposited Au on Cu for 10s (c), for 25s (d), for 45s (e), and for 1 min (f).

a relatively smoother surface than the bare Cu. Instead of sputter deposition, Au particles were deposited on the Cu surface using galvanic displacement with different deposition times in the range of 10-60 sec. In the case of 10 s deposition (Fig. 1(c)), Au particles with a size of 20 nm were formed on the surface, whose populations are much higher at the step edges. As the deposition time was increased to 25 s, as shown in Fig. 1(d), the population density of the Au particles rapidly rose without any significant growth of the particle size. Deposition for a longer time, *i.e.* 45 s (Fig. 1(e)), increased both the surface coverage and size (~50 nm) of the Au particles. However, there was only a slight increase in the surface coverage after deposition for 60 s (Fig. 1(f)), due to the self-limiting nature of the displacement reaction. It should be noted that even after a slight increase in the coverage, the deposit is still in the form of coalesced particles with significant amounts of exposed Cu on the surface.

The surface composition of the Au-modified electrodes was further examined by EPMA. The composition mapping of the Au-deposited (for 60 s) Cu electrode is shown in Figure 2. As clearly shown in the figure, Au is well distributed throughout the electrode and substantial amounts of the Cu substrate are still exposed. Considering that the penetration depth of the electron beam during the analysis is normally in the range of several tens of nanometers to several micrometers, it is not likely that the mapping results reflect the surface information only. However, the SEM images in Figure 1 and the EPMA analysis support the conclusion that the substrate Cu has a significant effect on the catalyst activity, that is, the electrochemical glucose oxidation on the Au-modified Cu electrode may exhibit some combined behaviors originating from both Au and Cu, as confirmed by the CV results. Another possible expectation from this structure is that there is electron movement between the adjacent Au and Cu atoms, due to the difference in their electronegativity (EN), *i.e.* electron transfer from Cu (EN=1.9) to Au (EN=2.4). Its role in the oxidation of glucose will be discussed in a later section.

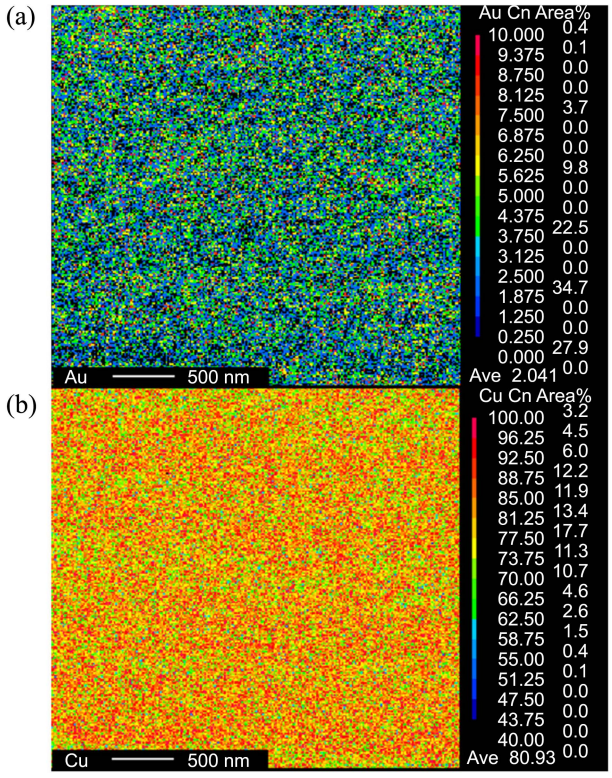

Figure 2. EPMA image of Au-modified Cu electrode by displacement deposition of Au for 1 min; (a) Au distribution and (b) Cu distribution.

The activities of the prepared electrodes, *viz.* Cu foil, Au deposited Cu foil prepared by sputter deposition, and Au modified Cu electrode prepared by displacement deposition, toward glucose oxidation were tested by CV in a glucose containing electrolyte. For comparison, the electrochemical behaviors of the three electrodes in the absence of glucose are shown in Figure 3. In the case of the Cu foil, distinct peaks corresponding to the formation of CuOH and $Cu(OH)_2$ are observed at −0.4 V and −0.2 V, respectively, during the forward scan. A more oxidized form of CuO(OH) is formed at potentials more positive than 0.7 V. During the backward scan, CuO(OH) is reduced to $Cu(OH)_2$ at 0.52 V. Further reductions to CuOH and Cu[20] are also monitored at −0.65 V and −0.9 V, respectively. However, in the case of the sputter deposited Au film, no such peaks related to Cu were observed and several peaks relevant to Au appeared.[22] A broad peak starting at −0.4 V was representing the formation of AuOH followed by further oxidation to form AuO. The generated oxidized species of Au were sequentially reduced back to AuOH and Au at 0.0 V and −0.25 V, respectively, during the backward scan.[22] Unlike the sputter deposited Au film on Cu, the Au-modified Cu prepared by displacement deposition exhibited much more complex behavior, resulting from the combined characteristics of Cu and Au. In detail, a peak was observed at −0.45 V corresponding to CuOH formation, whose tail was connected to a subsequent rapid current increase leading to two peaks at −0.2 V and −0.05 V corresponding to the generation of $Cu(OH)_2$ and AuOH, respectively. The presence of less noble Cu on the surface might

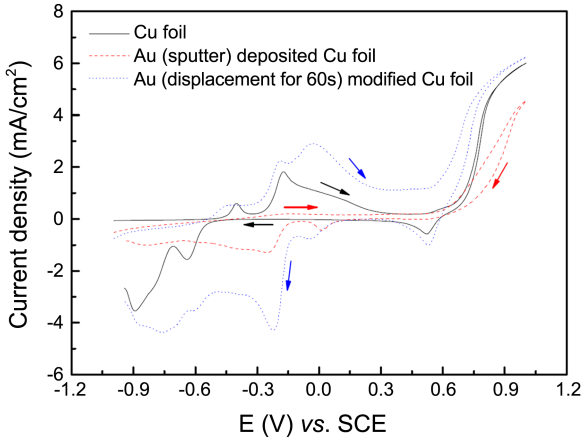

Figure 3. Cyclic voltammograms of various electrodes in the absence of glucose. The electrolyte is 0.3 M NaOH solution and the scan rate is 50 mV/s.

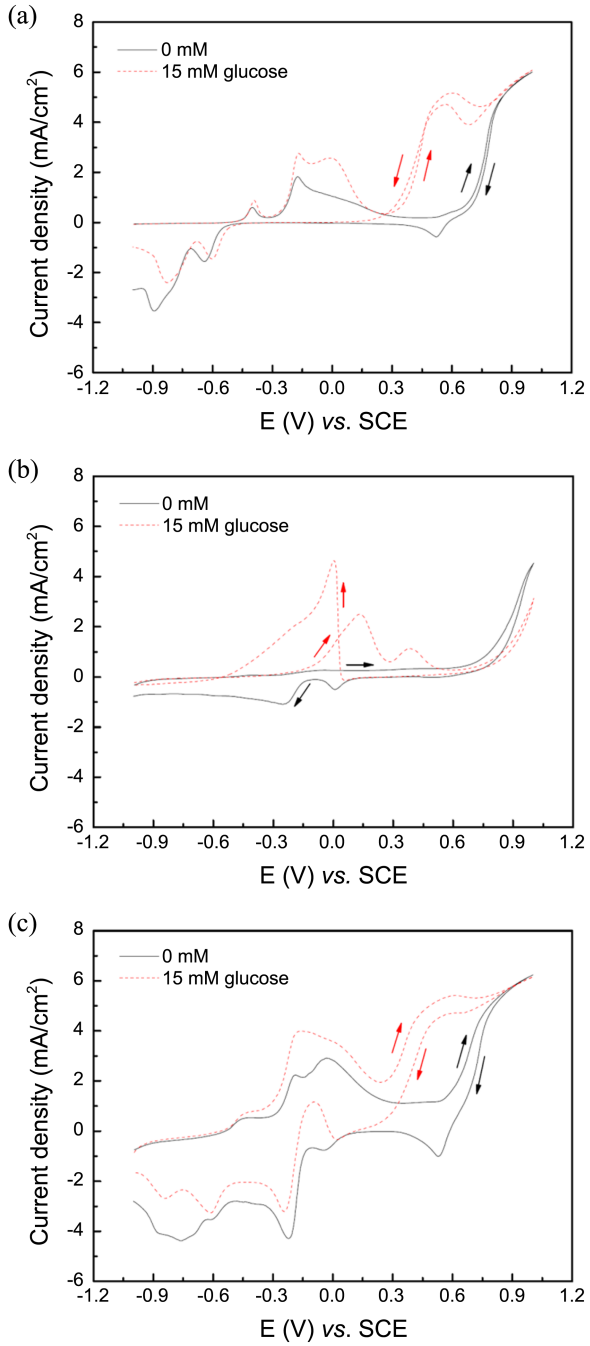

Figure 4. Cyclic voltammograms of glucose oxidation on various electrodes; (a) Cu foil, (b) sputter deposited Au film on Cu foil, (c) displacement deposited Au on Cu foil for 1 min. The electrolyte is composed of 0.3 M NaOH and 15 mM glucose. The voltammograms recorded in the glucose-free electrolyte are also added for comparison. The scan rate is 50 mV/s.

contribute to the shift of the AuOH peak in the positive direction as compared to that of the sputter deposited Au film on Cu. At potentials more positive than 0.6 V, the anodic currents were due to the formation of CuO(OH) and AuO. By changing the scan direction to backward, a series of reduction reactions were observed at 0.55 V, −0.05 V, −0.2 V, −0.6 V and −0.8 V, which corresponded to the reactions of CuO(OH) to $Cu(OH)_2$, AuO to AuOH, AuOH to Au, $Cu(OH)_2$ to CuOH and CuOH to Cu, respectively. As described in the previous section, this combined behavior is evidence that the Au-modified Cu electrode reveals characteristics of both Cu and Au, which would lead us to expect some synergistic effects on the glucose oxidation.

The activities of each electrode toward glucose oxidation were then tested in alkaline NaOH solution containing 15 mM of glucose by performing CV analysis and the results are presented in Figure 4. In the case of the Cu foil shown in Figure 4(a), distinctive differences in the peak shape and positions were observed. The broad peak at 0.0 V at the heel of the $Cu(OH)_2$ formation peak corresponds to the adsorption of glucose on the Cu surface. The adsorbed glucose starts to be oxidized at potentials more positive than 0.3 V, having a peak potential of 0.6 V. However, as shown in Figure 4(b), a different voltammogram for glucose oxidation on Au was observed on the sputter deposited Au film, which was in good accordance with the previous results on the glucose oxidation on Au.[32-34] The adsorption of glucose and subsequent oxidation to generate gluconolactone and gluconate[35] occurs at 0.1 V and 0.4 V, respectively. The sharp peak at around 0.0 V during the backward scan is probably due to the further oxidation of gluconolactone, which was preliminarily formed during the forward scan. If the surface of Cu is modified by Au particles deposited by displacement, the glucose oxidation characteristics are more like those of the Cu electrode than those of the Au sputter film, as shown in Figure 4(c). The combined peaks of hydroxide formation, glucose adsorption and its partial oxidation on both Cu and Au in Figures 4(a) and (b) are shown as a broad peak ranging from −0.2 V to 0.2 V. Its subsequent further oxidation starts at 0.25 V, having a peak potential of 0.6 V, which is very similar to that on Cu in Figure 4(a). The oxidation peak on Au at 0.4 V (see Fig. 4(b)) is probably buried in this peak. The oxidation continues during the backward scan after changing the scan direction at 1.0 V. If we compare the forward voltammogram with that on pure Cu, the glucose oxidation in this potential region has a more negative onset potential and higher current than that on the pure Cu electrode. For example, the oxidation current on the Au-modified Cu electrode at 0.4 V is about 2.7 mA/cm^2 higher than that on the pure Cu electrode. Most of the glucose oxidation at this potential is induced by CuO(OH), as discussed in the pure Cu case, however the Au particles still play important roles in the adsorption of glucose and its oxidation. In addition, unlike the sharp peak at 0.0 V in the case of the Au sputter film, the height of the oxidation peak of the preliminarily formed gluconolactone at around −0.1 V is decreased, which implies that the amount of reaction intermediate formed on the Au-modified Cu electrode is reduced.

The activity of the Au-modified Cu electrode was further investigated by varying the concentration of glucose. Figure 5(a) and (b) exhibit the forward I-V curves and chronoamperometry of the Au-modified Cu electrode prepared by displacement deposition for 1 min in the presence of 0 to 30 mM glucose. During the forward scan in Figure 5(a), the oxidation peaks in the range from 0.25 V to 0.7 V slightly

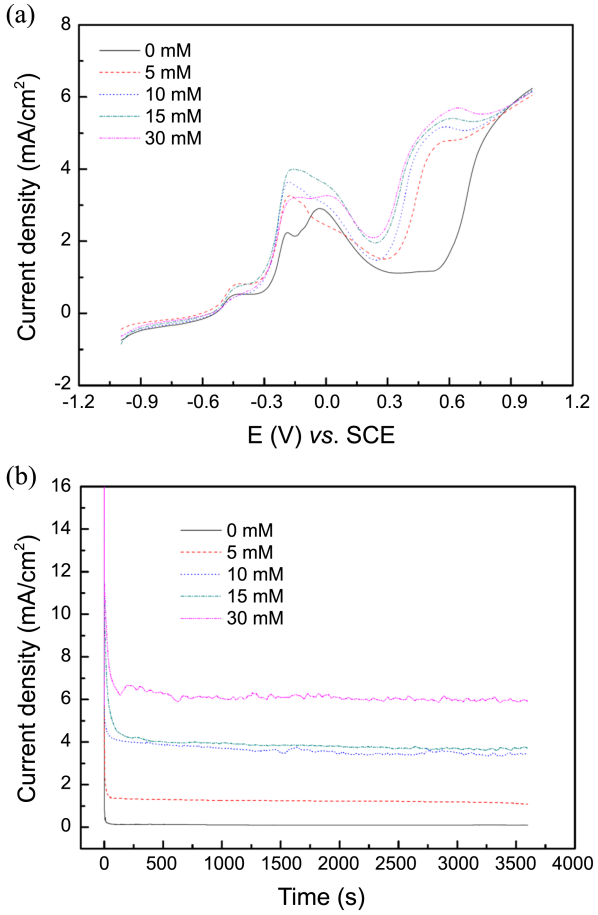

Figure 5. (a) Forward scan I-V curves (scan rate = 50 mV/s) and (b) chronoamperometry of glucose oxidation (0.6 V *vs*. SCE) on displacement deposited Au on Cu foil for 1 min with different concentrations of glucose. The electrolyte is composed of 0.3 M NaOH and various concentrations of glucose.

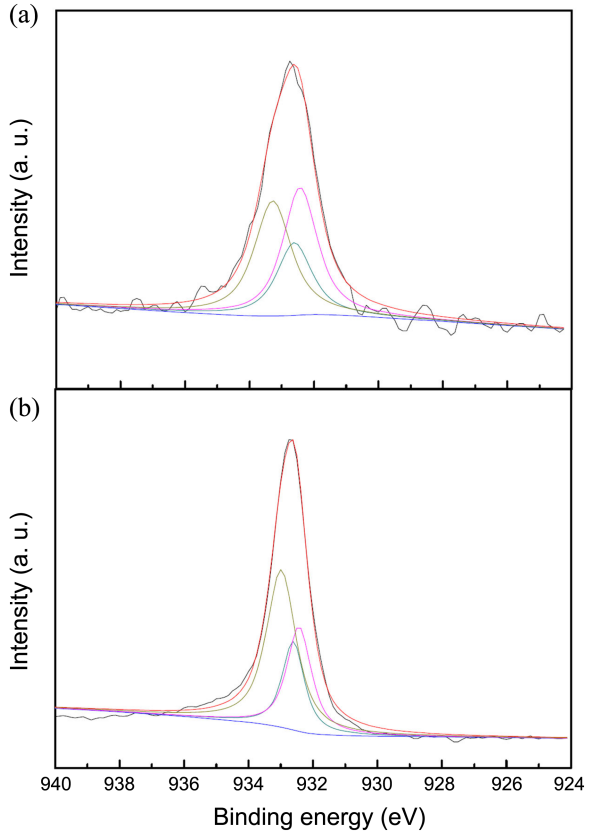

Figure 6. XPS analysis of Cu 2p binding energy; (a) Cu foil and (b) displacement deposited Au on Cu foil for 1 min.

increased with increasing glucose concentration, while the peaks in the range from –0.2 V to 0.2 V had no clear relationship with the glucose concentration. This is because multiple reactions of hydroxide formation, adsorption and oxidation of glucose occur simultaneously in this potential range. Therefore, the second oxidation peak in the potential range of 0.25 V to 0.7 V is a more suitable indicator for examining the activity of transition metal catalysts toward glucose oxidation. Based on this, chronoamperometry for glucose oxidation was performed at 0.6 V with different concentrations of glucose (Fig. 5(b)). As clearly shown in the figure, the current densities were gradually increased with increase in the glucose concentration, which implied that the potential range chosen above was successfully representing the glucose oxidation.

As mentioned above, the Au-modified Cu electrode exhibited better activity toward glucose oxidation than the pure Cu or Au film electrode. One of the reasons for this is the synergistic effects caused by the intrinsic activity of the Au nanoparticles. Besides this, we would expect the interactions between the adjacent Au and Cu on the electrode to have a positive impact. Figure 6 presents the Cu $2p_{3/2}$ XPS results from the Cu foil and Au-modified Cu electrodes. The Cu 2p peaks of the Cu foil (Fig. 6(a)) were observed at 932.6 eV, 932.4 eV and at 933.3 eV, which correspond to Cu^0, Cu^+ and Cu^{2+}, respectively.[36] This indicates that the Cu foil was composed of metallic Cu and native oxide. However, in the case of the Au-modified Cu electrode (Fig. 6(b)), the relative height of the Cu^{2+} peak was increased, while the Cu^0 and Cu^+ peaks were diminished. This implies that the oxidation state of Cu has been increased by the adjacent Au, due to electronegativity and, consequently, the Cu in the electrode became ready to oxidize the glucose.

As a final test, the stability of the Au-modified Cu electrode was investigated using chronoamperometry.[37] Figure 7 presents the chronoamperometry results of the Au-modified Cu electrodes with different displacement deposition times obtained in the 15 mM glucose containing electrolyte at 0.6 V for 3,600s. As clearly shown in the figure, while the Cu electrode exhibited a rapid decrease in the oxidation current immediately after the start of the experiment, the superior activity of the Au-modified Cu electrode was preserved at a current of about 3.5 mA/cm^2 during the experiments, suggesting the enhanced activity and stability of the latter electrode. However, for practical applicability to BFCs, it is necessary to consider the stability of Cu-based catalyst in physiological condition (*i.e.*, blood pH 7.2). The reported bio-cathode open circuit potential (OCP) in phosphate buffer (0.1 M, pH 7, 20 °C) was 0.5-0.6 V *vs*. SCE.[38] Considering

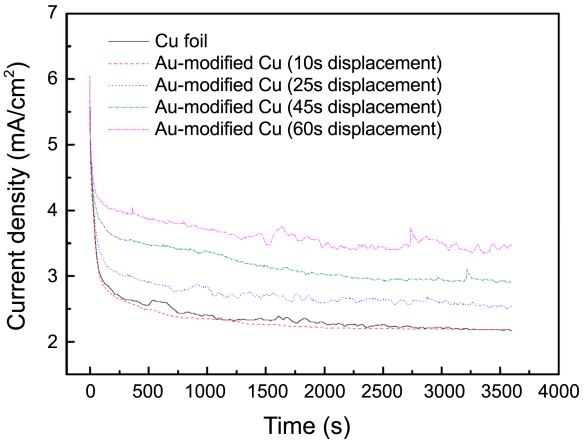

Figure 7. Chronoamperometry of glucose oxidation at 0.6 V (*vs.* SCE) according to the type of electrode. The electrolyte is composed of 0.3 M NaOH and 10 mM glucose.

that the OCP of glucose BFC is normally in the range of 0.7 V-0.5 V,[39-41] the anode OCP is roughly supposed to be value around −0.2~0.1 V *vs*. SCE. The anode potential might be more positive at the typical operation voltage of biofuel cell and long term operation at this pH and potential might cause the stability issue of Cu.

Conclusion

A galvanic displacement deposition method was used for the fabrication of an Au-modified Cu electrode for glucose oxidation. The morphology and composition of the Au-modified Cu electrode were characterized and it was found that spherical nano-sized Au particles were well dispersed on the Cu electrode, exposing both the Au and Cu surfaces to the test environment. The activities of the fabricated electrodes toward glucose oxidation were tested using electrochemical analysis and compared with those of a pure Cu foil electrode and sputter deposited Au film on Cu foil. While the Cu foil and sputter deposited Au film exhibited their inherent behavior during the glucose oxidation, the Au-modified Cu electrode exhibited better activity, characterized by a negative shift in the oxidation potential and increased oxidation current. Besides the aid of the intrinsic activity of Au, the electron transfer from Cu to the adjacent Au and resulting increase in the oxidation state of Cu are considered to be important reasons for the enhanced activity. The superior stability of the Au-modified Cu electrode was also confirmed by the chronoamperometry test.

Acknowledgments. This research was supported by Chung-Ang University Research Scholarship Grants in 2012.

References

1. Barton, S. C.; Gallaway, J.; Atanassov. P. *Chem. Rev.* **2004**, *104*, 4867.
2. Heller, A. *Phys. Chem. Chem. Phys.* **2004**, *6*, 212.
3. Bullen, R. A.; Arnot, T. C.; Lakeman, J. B.; Walsh, F. C. *Biosens. Bioelectron.* **2006**, *21*, 2015.
4. Kerzenmarcher, S.; Ducreee, J.; Zengerle, R.; von Stetetten, F. *J. Power Sources* **2008**, *182*, 1.
5. Deng, C.; Chen, J.; Chen, X.; Xiao, C.; Nie, L.; Yao, S. *Biosens. Bioelectron.* **2008**, *23*, 1272.
6. Safavi, A.; Maleki, N.; Farjami, E. *Biosens. Bioelectron.* **2009**, *24*, 1655.
7. Rong, L.-Q.; Yang, C.; Qian, Q.-Y.; Xia, X.-H. *Talanta* **2007**, *72*, 819.
8. Luque, G. L.; Rodriguez, M. C.; Rivas, G. A. *Talanta* **2005**, *66*, 467.
9. Wilson, R.; Turner, A. P. F. *Biosens. Bioelectron.* **1992**, *7*, 165.
10. Park, S.; Boo, H.; Chung, T. D. *Anal. Chim. Acta* **2006**, *556*, 46.
11. Mahshid, S. S.; Mahshid, S.; Dolati, A.; Ghorbani, M.; Yang, L.; Luo, S.; Cai, Q. *Electrochim. Acta* **2011**, *58*, 551.
12. Sun, Y.; Buck, H.; Mallouk, T. E. *Anal. Chem.* **2001**, *73*, 1599.
13. Jin, C.; Chen, Z. *Synthetic Met.* **2007**, *157*, 592.
14. Tominaga, M.; Shimazoe, T.; Nagachima, M.; Taniguchi, I. *Journal of Electroanal. Chem.* **2008**, *615*, 51.
15. Aoun, S. B.; Dursun, Z.; Sotomura, T.; Taniguch, I. *Electrochem. Commun.* **2004**, *6*, 742.
16. Habrioux, A.; Sibert, E.; Servat, K.; Vogel, W.; Kokoh, K. B.; Alonso-Vante, N. *J. Phys. Chem. B* **2007**, *111*, 10329.
17. Iwasita, T.; Hoster, H.; John-Anacker, A.; Lin, W. F.; Vieltich, W. *Langmuir* **2000**, *16*, 522.
18. Cui, H.-F.; Ye, J.-S.; Liu, X.; Zhang, W.-D.; Sheu, F.-S. *Nanotechnology* **2006**, *17*, 2334.
19. Tominaga, M.; Nagashima, M.; Nishiyama, K.; Taniquchi, I. *Electrochem. Commun.* **2007**, *9*, 1892.
20. Hassan, H. B.; Hamid, Z. A. *Int. J. Electrochem. Sci*. **2011**, *6*, 5741.
21. Jafarian, M.; Forouzandeh, F.; Danaee, I.; Gobal, F. *J. Solid State Electrochem.* **2009**, *13*, 1171.
22. Bai, Y.; Yang, W.; Sun, Y.; Sun, C. *Sensor. Actuat. B: Chem.* **2008**, *134*, 471.
23. Ho, S.-W.; Su, Y.-S. *J. Catal.* **1997**, *168*, 51.
24. Ahmadi, T. S.; Wang, Z. L.; Green, T. C.; Henglein, A.; El-Sayed, M. A. *Science* **1996**, *272*, 1924.
25. Kim, H.; Subramanian, N. P.; Popov, B. N. *J. Power Sources* **2004**, *138*, 14.
26. Duarte, M. M. E.; Pilla, A. S.; Sieben, J. M.; Mayer, C. E. *Electrochem. Commun.* **2006**, *8*, 159.
27. Hu, Y.; Jin, J.; Wu, P.; Zhang, H.; Cai, C. *Electrochim. Acta* **2010**, *56*, 491.
28. Alvisi, M.; Galtieri, G.; Giorgi, L.; Giorgi, R.; Serra, E.; Signore, M. A. *Surf. Coat. Technol.* **2005**, *200*, 1325.
29. Strasser, P.; Fan, Q.; Devenney, M.; Weinberg, W. H. *J. Phys. Chem. B* **2003**, *107*, 11013.
30. Zeng, J.; Yang, J.; Lee, J. Y.; Zhou, W. *J. Phys. Chem. B* **2006**, *110*, 24606.
31. Wang, D.; Xin, H. L.; Yu, Y.; Wang, H.; Rus, E.; Muller, D. A.; Abruna, H. D. *J. Am. Chem. Soc*. **2010**, *132*, 17664.
32. Wang, J.; Gong, J.; Xiong, Y.; Yang, J.; Gao, Y.; Liu, Y.; Lu, X.; Tang, Z. *Chem. Commun*. **2011**, *47*, 6894.
33. Pasta, M.; Ruffo, R.; Falletta, E.; Mari, C. M.; Della Pina, C. *Gold Bull*. **2010**, *43*, 57.
34. Ivanov, I.; Vidakovic, T. R.; Sundmacher, K. *Chem. Biochem. Eng. Q* **2009**, *23*, 77.
35. Pasta, M.; Mantia, F. L.; Cui, Y. *Electrochim. Acta* **2010**, *55*, 5561.
36. Wagner, C. D.; Naumkin, A. V.; Kraut-Vass, A.; Allison, J. W.; Powell, C. J.; Rumble, J. R., Jr. *NIST Standard Reference Database 20, Version 3.4 (web version) (http:/srdata.nist.gov/xps/)*, 2003.
37. Basu, D.; Basu, S. *Int. J. Hydrogen Energy* **2011**, *36*, 14923.
38. Zebda, A.; Gondran, C.; Goff, A. L.; Holzinger, M.; Cinquin, P.; Cosnier, S. *Nat. Commun.* **2011**, 2:370 doi: 10.1038/ncomms1365.
39. Shim, J.; Kim, G.-Y.; Moon, S.-H. *J. Electroanal. Chem.* **2011**, *653*, 14.
40. Schubart, I. W.; Gobel, G.; Lisdat, F. *Electrochim. Acta* **2012**, *82*, 224.
41. Zebda, A.; Gondran, C.; Cinquin, P.; Cosnier, S. *Sensor. Actuat. B: Chem.* **2012**, *173*, 760.